Contribution from the Department of Chemistry,
Purdue University, West Lafayette, Indiana 47907

Direct Determination of Self-Exchange Electron-Transfer Rate Constants of Nickel(III,II) Complexes by ^{61}Ni EPR Line Broadening

Jean-Fu Wang, Krishan Kumar, and Dale W. Margerum*

Received September 29, 1988

A novel method, based on the influence of ^{61}Ni on the room-temperature electron paramagnetic resonance spectra of Ni(III) complexes, is used for the measurement of electron-transfer self-exchange rate constants of nickel(III,II) complexes. An electron-transfer self-exchange rate constant (k_{11} = 450 ± 50 M^{-1} s^{-1} at 24 °C) is measured for the $Ni^{III}(H_{-2}Aib_3)(H_2O)_2$ and $Ni^{II}(H_{-2}Aib_3)^-$ couple, where Aib_3 is the tripeptide of α-aminoisobutyric acid and H_{-2} designates two deprotonated-N(peptide) groups. This k_{11} value reflects an inner-sphere enhancement attributed to bridging by an axial water molecule. The exchange rate decreases when pyridine replaces one of the axial water molecules of the nickel(III) complex. The electron-transfer rate constant between $Ni^{III}(H_{-2}Aib_3)(py)(H_2O)$ and $Ni^{II}(H_{-2}Aib_3)^-$ is 103 ± 8 M^{-1} s^{-1} at 23 °C.

Introduction

Self-exchange electron-transfer rate constants (k_{11}) are difficult to measure directly because no net reaction occurs. As a result, k_{11} values are sometimes calculated indirectly from cross-exchange reactions by using Marcus' theory.[1,2] In such cases it is vital that the outer-sphere criterion be met. Direct measurements by isotopic labeling or other techniques are essential to give reliable reference values. (i) Isotopic labeling with rapid separation was used to measure k_{11} values for the $Fe(CN)_6^{3-}/Fe(CN)_6^{4-}$ couple[3] and the $IrCl_6^{2-}/IrCl_6^{3-}$ couple.[4,5] (ii) NMR line broadening, performed by addition of small amounts of paramagnetic species to solutions of diamagnetic species, has been used for a few couples.[6,7] This method was used to measure k_{11} for the $Cu^{III}(H_{-2}Aib_3)/Cu^{II}(H_{-2}Aib_3)(H_2O)_2^-$ couple.[8] (iii) Derivative NMR line width techniques were used for the Cu(II)/Cu(I) couple in concentrated HCl.[9] (iv) NMR line shape[6] can be used to determine k_{11} in complexes where the NMR peaks are affected by spin–spin coupling from adjacent protons of coordinated ligands. Contact shifts and the broadening of the NMR peaks due to the paramagnetic form of the complexes are fitted to the line shape. This technique was used for the $Fe(4,7\text{-}Me_2phen)_3^{3+,2+}$ couple. (v) Transfer diffusion[10] was used to determine k_{11} for the $Fe(phen)_3^{3+}/Fe(phen)_3^{2+}$ couple by measuring the apparent diffusion coefficient of $Fe(phen)_3^{2+}$ electrochemically. (vi) Near-infrared spectroscopy[11] was used to determine the k_{11} value for the $Ru(NH_3)_6^{2+}/Ru(NH_3)_6^{3+}$ couple by taking advantage of the change in absorbance when the deuterium form, $Ru(ND_3)_6^{3+}$, reacted with the proton form of $Ru(NH_3)_6^{2+}$. (vii) EPR line broadening, performed by addition of a diamagnetic species to the solution of a radical species, was used in the case of the naphthalene/naphthalene negative ion couple.[12] (viii) Freeze-quenched EPR spectra of $Ni^{III}(cyclam)(H_2O)_2^{3+}$ after exchange with $^{61}Ni^{II}(cyclam)^{2+}$ were used to measure this electron-transfer reaction.[13] All the methods have some disadvantages and frequently are limited to a few types of chemical systems. Isotopic labeling depends on the availability of rapid separation methods that do not induce exchange. The freeze-quench method requires slow electron transfer relative to the speed of freezing the solution. It also requires careful calibration of the EPR tubes and highly reproducible positioning in the EPR spectrometer in order to obtain quantitative information about the quartet of the ^{61}Ni peaks in the $g_\parallel$ region relative to the natural Ni signal.

In this work we report a new method to measure rate constants for electron-transfer reactions of Ni(III,II) complexes in solution. We find that ^{61}Ni ($I = {}^3/_2$) broadens the width (and decreases the intensity) of the first-derivative EPR signal in proportion to its concentration in the Ni(III) complex. As a result, exchange reactions can be followed without freezing the solution. This permits the study of faster reactions with much greater precision. It may be possible to extend this method to other metal complexes.

Stabilization of trivalent copper and nickel is no longer considered unusual. Chemical or electrochemical oxidation of nickel(II) and copper(II) deprotonated-peptide complexes give the corresponding nickel(III) and copper(III) complexes, which are moderately stable in aqueous media.[14–18] Direct determination of a self-exchange electron-transfer rate constant (k_{11}) requires a set of solution conditions where both species of the redox couple are stable. Unusually stable Cu(III)–tripeptide and Ni(III)–tripeptide complexes are derived from α-aminoisobutyric acid (Aib): $Cu^{III}(H_{-2}Aib_3)$ and $Ni^{III}(H_{-2}Aib_3)(H_2O)_2$ (H_{-2} designates two deprotonated-N(peptide) groups that are coordinated to the metal).[18] For the $Cu^{III}(H_{-2}Aib_3)/Cu^{II}(H_{-2}Aib_3)(H_2O)_2^-$ couple, the electron-transfer self-exchange rate constant was determined by a ^{1}H NMR line-broadening technique.[8] However, for the $Ni^{III}(H_{-2}Aib_3)(H_2O)_2/Ni^{II}(H_{-2}Aib_3)^-$ couple (structure I and

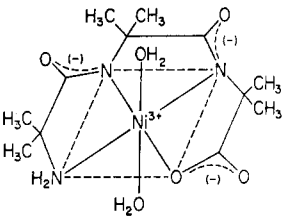

I ($Ni^{III}(H_{-2}Aib_3)(H_2O)_2$)

structure II), the electron-transfer reaction was so slow that no

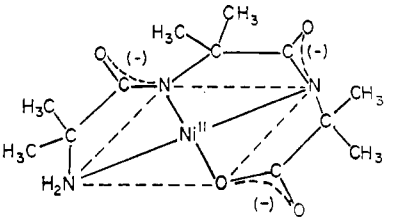

II ($Ni^{II}(H_{-2}Aib_3)^-$)

line broadening was observed by the NMR technique.[19] The

(1) Marcus, R. A. *J. Phys. Chem.* **1963**, *67*, 853–857.
(2) Marcus, R. A. *Annu. Rev. Phys. Chem.* **1964**, *15*, 155–196.
(3) Campion, R. J.; Deck, C. F.; King, P., Jr.; Wahl, A. C. *Inorg. Chem.* **1967**, *6*, 672–681.
(4) Hurwitz, P.; Kustin, K. *Trans. Faraday Soc.* **1966**, *62*, 427–432.
(5) Sloth, E. N.; Garner, C. S. *J. Am. Chem. Soc.* **1955**, *77*, 1440–1444.
(6) Chan, M. S.; Wahl, A. C. *J. Phys. Chem.* **1978**, *82*, 2542–2549.
(7) Dietrich, M. W.; Wahl, A. C. *J. Chem. Phys.* **1963**, *38*, 1591–1596.
(8) Koval, C. A.; Margerum, D. W. *Inorg. Chem.* **1981**, *20*, 2311–2318.
(9) McConnel, H. M.; Weaver, H. E. *J. Chem. Phys.* **1956**, *25*, 307–311.
(10) Ruff, I.; Zimonyi, M. *Electrochim. Acta* **1973**, *18*, 515–516.
(11) Meyer, T. J.; Taube, H. *Inorg. Chem.* **1968**, *7*, 2369–2379.
(12) Ward, R. L.; Weissman, S. I. *J. Am. Chem. Soc.* **1957**, *79*, 2086–2090.
(13) McAuley, A.; Macartney, D. H.; Oswald, T. *J. Chem. Soc., Chem. Commun.* **1982**, 274–275.
(14) Margerum, D. W.; Chellappa, K. L.; Bossu, F. P.; Burce, G. L. *J. Am. Chem. Soc.* **1975**, *97*, 6894–6896.
(15) Bossu, F. P.; Margerum, D. W. *J. Am. Chem. Soc.* **1976**, *98*, 4003–4004.
(16) Bossu, F. P.; Margerum, D. W. *Inorg. Chem.* **1977**, *16*, 1210–1214.
(17) Neubecker, T. A.; Kirksey, S. T., Jr.; Chellappa, K. L.; Margerum, D. W. *Inorg. Chem.* **1979**, *18*, 444–448.
(18) Kirksey, S. T., Jr.; Neubecker, T. A.; Margerum, D. W. *J. Am. Chem. Soc.* **1979**, *101*, 1631–1633.

0020-1669/89/1328-3481$01.50/0

failure to see line broadening indicated that the self-exchange rate constant must be less than 800 M^{-1} s^{-1}.[19] In addition, an electron-transfer self-exchange rate constant for $Ni^{III,II}(H_{-2}Aib_3)^{0,-}$ was predicted[19] to be 550 ± 150 M^{-1} s^{-1} on the basis of many $Ni^{III,II}(H_{-2}Aib_3)^{0,-}$ cross-reactions with $Ni^{III,II}(H_{-n}L)$, where L is the peptide ligand.

The reaction investigated is given in eq 1. This exchange reaction was chosen as a model system because of the above

$$^{61}Ni^{III}(H_{-2}Aib_3)(H_2O)_2 + Ni^{II}(H_{-2}Aib_3)^- \underset{}{\overset{k_{11}}{\rightleftharpoons}} {}^{61}Ni^{II}(H_{-2}Aib_3)^- + Ni^{III}(H_{-2}Aib_3)(H_2O)_2 \quad (1)$$

preliminary information and because of the excellent kinetic stability of $Ni^{III}(H_{-2}Aib_3)(H_2O)_2$ relative to equatorial substitution reactions, to acid attack, and to acid-catalyzed intramolecular redox decomposition.[18] The $Ni^{II}(H_{-2}Aib_3)^-$ complex also is relatively stable. It dissociates more slowly in acid than is the case for other Ni(II) peptides.[20,21] These properties make the Aib_3 complexes very suitable for the study of Ni(III,II) electron-transfer reactions. The self-exchange rate constant was determined from the difference in the room-temperature EPR line broadenings of $Ni^{III}(H_{-2}Aib_3)(H_2O)_2$ and $^{61}Ni^{III}(H_{-2}Aib_3)(H_2O)_2$ by use of an EPR stopped-flow mixing and data acquisition system.[22]

The EPR spectra of many nickel(III) complexes in frozen aqueous solutions are characteristic of an elongated tetragonal geometry with $g_\perp > g_\parallel$ in accord with an unpaired electron located in the d_{z^2} orbital.[23,24] For ^{61}Ni, a quartet splitting pattern is seen in the $g_\parallel$ region.[13,25]

Experimental Section

Reagents. The tripeptide of α-aminoisobutyric acid (Aib_3), was prepared by H. D. Lee by use of previously reported procedures.[18] Nickel(II) perchlorate, prepared from $NiCO_3$ and $HClO_4$, was recrystallized, and its solutions were standardized by EDTA titration with murexide indicator. Enriched ^{61}Ni (88.84%) was obtained as the metal (Oak Ridge National Laboratory) and was converted to $^{61}Ni(NO_3)_2$ by dissolution of the metal in 0.05 M HNO_3. The solutions of $Ni^{II}(H_{-2}Aib_3)^-$ and $^{61}Ni^{II}(H_{-2}Aib_3)^-$ (ca. 5 × 10^{-3} M) were prepared by the reaction of $Ni(ClO_4)_2$ or $^{61}Ni(NO_3)_2$ with a 10–15% excess of the peptide. These solutions were raised to pH 10 by the addition of NaOH over the period of 3–8 h. The ionic strength of all solutions was adjusted to 0.1 with $NaClO_4$.

The $Ni^{III}(H_{-2}Aib_3)/^{61}Ni^{III}(H_{-2}Aib_3)$ solutions were prepared by electrochemical oxidation of the corresponding Ni^{II} complexes (the solutions were adjusted to pH 7 immediately prior to oxidation) at 0.84 V vs a Ag/AgCl reference electrode with use of a flow bulk electrolysis column.[19] The nickel(III) peptide solutions were stored in the dark under slightly acidic conditions (pH ≃4) in order to minimize redox decomposition. The concentration of total Ni(III) was determined after dilution by measuring the absorbance at 352 nm (ε = 3800 M^{-1} cm^{-1}).[26] The concentration of $Ni^{II}(H_{-2}Aib_3)^-$ was confirmed by measuring the absorbance at 415 nm (ε = 250 M^{-1} cm^{-1}).[21]

Mixed-ligand complex solutions were prepared by the reaction of $^{61}Ni^{III}(H_{-2}Aib_3)$ with solutions of pyridine (0.45–1.5 M) adjusted to pH 6.50. Since the $^{61}Ni^{III}(H_{-2}Aib_3)$ complex decomposes slowly in the presence of pyridine, the mixed-ligand complex solutions were prepared just prior to the kinetic experiments. $[^{61}Ni^{III}(H_{-2}Aib_3)]_T$ was corrected by comparing the absorbance of this complex with a decay plot of $Ni^{III}(H_{-2}Aib_3)$ mixed with pyridine. The time elapsed from the beginning of the preparation of the mixed-ligand complex solutions until the completion of the self-exchange reactions ranged from 16 to 60 min, and the concentration corrections ranged from 0.2 to 1.2%.

Measurements. Room-temperature EPR spectra were obtained at 9.40 GHz with a Varian E-109 X-band EPR spectrometer modulated at 100 kHz. The data were acquired and manipulated by a Varian E-935 EPR data acquisition system. The data acquisition time of this system can be varied from 16 ms to 30 s in the rapid-scan external triggering mode and from 30 to 17 000 s in the magnet scan mode. The magnetic field was calibrated relative to α,α′-diphenyl-β-picrylhydrazyl (DPPH), g_{iso} = 2.0037.[27] A hand-driven pushblock, which simultaneously drives two 10-mL glass syringes, delivers the solutions into a quartz mixing/observation cell (Model WG-804 Wilmad). This cell is positioned in a Varian 238 multipurpose cavity. Only 2–3 mL of each reagent is consumed per experiment. The flow is stopped at the drive syringes in order to minimize stress and mechanical vibration on the mixing/observation cell. A microswitch with an adjustable trigger point is located on the syringe drive pushblock to activate the data acquisition.[22]

EPR spectra of frozen aqueous solutions were recorded at −150 °C and at 9.08 GHz with a Varian E-231 variable-temperature cavity and a Varian E-238 variable-temperature controller.

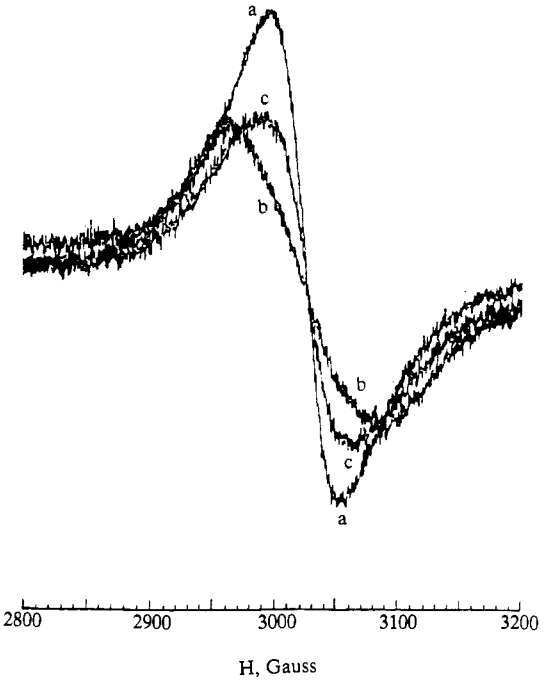

Figure 1. EPR spectra at 24 °C: (a) $Ni^{III}(H_{-2}Aib_3)$ (0.845 mM, pH 7.0, 0.1 M phosphate buffer); (b) $^{61}Ni^{III}(H_{-2}Aib_3)$ (0.671 mM, pH 7.0, 0.1 M phosphate buffer); (c) a mixture of equal volumes of $^{61}Ni^{III}(H_{-2}Aib_3)$ (1.342 mM, pH 2.25) and $Ni^{II}(H_{-2}Aib_3)^-$ (2.00 mM, pH 10.0). The microwave power was 30 mW, microwave frequency 9.40 GHz, modulation amplitude 12.5 G, modulation frequency 100 kHz, time constant 0.032 s, receiver gain 1.25 × 10^4.

Table I. Line Broadening of $Ni^{III}(H_{-2}Aib_3)$ as a Function of Percent ^{61}Ni

% $^{61}Ni^{III}(H_{-2}Aib_3)$	ΔH_{pp}, G	rel intens of EPR signal at 2990 G[a]
1.13[b]	65	57 ± 1
36.35	80	47 ± 1
88.84	125	29 ± 1

[a] Normalized to $[^{61}Ni^{III}(H_{-2}Aib_3)] + [Ni^{III}(H_{-2}Aib_3)] = 0.671$ mM. [b] Natural abundance.

^{61}Ni EPR Line Broadening. The room-temperature EPR signal of $Ni^{III}(H_{-2}Aib_3)$ broadens as the percentage of the ^{61}Ni isotope increases, as shown in Figure 1. The peak-to-peak width of the first-derivative EPR signal (ΔH_{pp}) as a function of the percent ^{61}Ni is given in Table I. The EPR signal intensity at 2990 G (Figure 1) decreases as the ^{61}Ni content increases, and data in Table I show that this signal is proportional to the percent ^{61}Ni. The amplitudes of derivative EPR signals have been used previously to measure the concentration of paramagnetic species in equilibrium studies[28] and in kinetic studies.[22,29] In the present case, the amplitude is used as a measure of the isotopic composition of a para-

(19) Murray, C. K.; Margerum, D. W. *Inorg. Chem.* **1983**, *22*, 463–469.
(20) Owens, G. D.; Phillips, D. A.; Czarnecki, J. J.; Raycheba, J. M. T.; Margerum, D. W. *Inorg. Chem.* **1984**, *23*, 1345–1353.
(21) Kennedy, W. R.; Margerum, D. W. *Inorg. Chem.* **1985**, *24*, 2490–2495.
(22) Jacobs, S. A.; Kramer, G. W.; Santini, R. E.; Margerum, D. W. *Anal. Chim. Acta* **1984**, *157*, 117–124.
(23) Lappin, A. G.; Murray, C. K.; Margerum, D. W. *Inorg. Chem.* **1978**, *17*, 1630–1634.
(24) Haines, R. I.; McAuley, A. *Coord. Chem. Rev.* **1981**, *39*, 77–119.
(25) Pappenhagen, T. L.; Margerum, D. W. *J. Am. Chem. Soc.* **1985**, *107*, 4576–4577.
(26) Murray, C. K. Ph.D. Thesis, Purdue University, 1982.
(27) Swartz, H. M.; Bolton, J. R.; Borg, D. C. *Biological Applications of Electron Spin Resonance*; Wiley-Interscience, a Division of John Wiley and Sons, Inc.: New York, 1972; p 101.
(28) Pappenhagen, T. L.; Kennedy, W. R.; Bowers, C. P.; Margerum, D. W. *Inorg. Chem.* **1985**, *24*, 4356–4362.
(29) Klimes, N.; Lassmann, G.; Ebert, B. *J. Magn. Reson.* **1980**, *37*, 53–59.

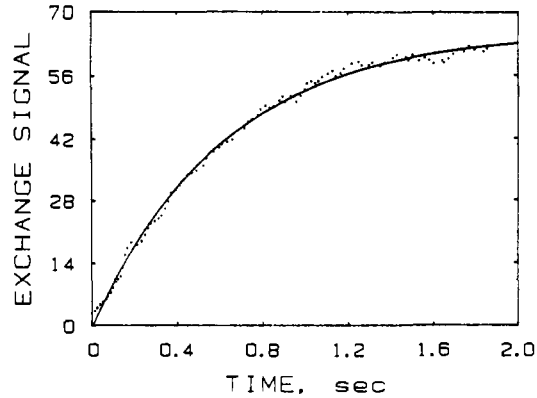

Figure 2. First-order nonlinear regression fit of the electron-transfer self-exchange signal between $^{61}Ni^{III}(H_{-2}Aib_3)$ (2.64 mM, pH 4) and $Ni^{II}(H_{-2}Aib_3)^-$ (5.00 mM, pH 10). The points are experimental, and the curve is calculated from eq 2. The magnetic field was 2990 G, microwave power 65 mW, microwave frequency 9.402 GHz, modulation amplitude 40 G, modulation frequency 100 kHz, time constant 0.016 s, and receiver gain 1.0×10^4.

magnetic species as a function of time.

The self-exchange rate was monitored at 2990 G. Equal volumes of $Ni^{II}(H_{-2}Aib_3)^-$ [(2–5) $\times 10^{-3}$ M, pH 10] and $^{61}Ni^{III}(H_{-2}Aib_3)$ [(0.6–3) $\times 10^{-3}$ M, pH 4] solutions were mixed by rapid flow into the EPR cell.[22] The amplitude of the first-derivative EPR signal vs time was monitored and recorded by the Varian E-935 EPR data acquisition system. Figure 2 shows a first-order nonlinear regression curve for a representative electron-transfer self-exchange signal in accord with eq 2.

$$S_t = S_\infty - (S_\infty - S_0)\exp(-k_{obsd}t) \quad (2)$$

In the presence of pyridine, equal volumes of mixed-ligand solution (0.76×10^{-3} M $[^{61}Ni^{III}(H_{-2}Aib_3)]_T$, pH 6.50) and $Ni^{II}(H_{-2}Aib_3)^-$ (2.7×10^{-3} M, pH 10) were reacted in the EPR stopped-flow mixer. The magnetic field was fixed at 3045 G, and the self-exchange signal was recorded as before.

Treatment of Data. The logarithmic form of the first-order exchange law of eq 1 is the McKay relationship[30] (eq 3), where $C_A = [Ni(III)]_T$

$$\ln(1 - F) = -R_{ex}\left(\frac{C_A + C_X}{C_A C_X}\right)t \quad (3)$$

$= [Ni^{III}(H_{-2}Aib_3)] + [^{61}Ni^{III}(H_{-2}Aib_3)]$, $C_X = [Ni(II)]_T = [Ni^{II}(H_{-2}Aib_3)^-] + [^{61}Ni^{II}(H_{-2}Aib_3)^-]$, F = fraction of exchange at time t, and $R_{ex} = k_{11}C_AC_X$, which is the rate of the exchange reaction between $^{61}Ni^{III}(H_{-2}Aib_3)$ and $Ni^{II}(H_{-2}Aib_3)^-$.

Equation 4 defines F, where S_0 is the initial amplitude of the EPR signal, S_t is the amplitude of EPR signal at time t, and S_∞ is the equi-

$$F = \frac{S_t - S_0}{S_\infty - S_0} \quad (4)$$

librium amplitude. The S_∞ value was obtained with a simplex curve fitting method.[31,32] Upon substitution of eq 4 into eq 3, the McKay equation can be written as eq 5. Plots of $\ln(S_\infty - S_t)$ vs time are linear

$$\ln\left(\frac{S_\infty - S_t}{S_\infty - S_0}\right) = -k_{11}(C_A + C_X)t \quad (5)$$

$$\ln(S_\infty - S_t) = -k_{11}(C_A + C_X)t + \ln(S_\infty - S_0) \quad (6)$$

with slope $= -k_{11}(C_A + C_X)$. Therefore, the self-exchange rate constant $k_{11} = -(\text{slope})/(C_A + C_X)$ can be determined.

Results and Discussion

Self-Exchange Rate Constants for Ni(III,II) Complexes. The electron-transfer self-exchange rate constants of $Ni^{III}(H_{-2}Aib_3)(H_2O)_2/Ni^{II}(H_{-2}Aib_3)^-$ for five trials in aqueous solution are reported in Table II. For each individual trial, the parameters in Table II were calculated by linear regression.[33] The mean value

Table II. Data for the Electron-Transfer Self-Exchange Reaction of $Ni^{III}(H_{-2}Aib_3)(H_2O)_2/Ni^{II}(H_{-2}Aib_3)^-$ in Aqueous Solution[a]

10^3C_A, M	10^3C_X, M	−(slope), s^{-1}	k_{11},[b] M^{-1} s^{-1}
1.32	2.50	1.56 ± 0.02	408 ± 5
1.32	2.50	1.64 ± 0.04	430 ± 10
1.32	2.50	1.68 ± 0.05	440 ± 10
0.342	1.00	0.62 ± 0.02	460 ± 10
0.342	1.00	0.71 ± 0.02	530 ± 10
			mean 450 ± 50

[a] 2990 G, 24 ± 1 °C, μ = 0.1, $C_A = [Ni(III)]_T$, $C_X = [Ni(II)]_T$, slope equals $-k_{11}(C_A + C_X)$. Uncertainties are one standard deviation.

of k_{11} is 450 ± 50 M^{-1} s^{-1}. This is in good agreement with previous estimates[19] of the self-exchange rate constant for eq 1.

It should be noted that the two reactants do not have identical compositions, because the Ni(III) complex has two axial waters coordinated in an elongated tetragonal structure whereas the Ni(II) complex has a square-planar geometry.[21] A change in coordination would be expected for one or both reactants prior to an outer-sphere electron-transfer process, because both Ni(III) and Ni(II) should have the same number of coordinated water molecules (i.e. 0, 1, or 2) in the transition state. A similar situation was found for the $Cu^{III}(H_{-2}Aib_3)$ exchange with $Cu^{II}(H_{-2}Aib_3)(H_2O)_2^-$.[8] Changes of coordination number also must be considered for the exchange reactions between $Ni^{III}(cyclam)(H_2O)_2^{3+}$ and $Ni^{II}(cyclam)^{2+}$ as well as for the Cu(II)/Cu(I) couple in concentrated HCl.

Several types of Ni(III,II) peptide reactions with other redox couples have been studied. (1) In cases such as $Fe(CN)_6^{3-,4-}$, where the reaction partner can form an axial inner-sphere bridge with the nickel complexes, the reactions are extremely fast.[34] These are inner-sphere reactions where cyanide is bridged between the $Fe^{III,II}$ and $Ni^{III,II}$ metal centers. The apparent k_{11} values are as large as 10^7 M^{-1} s^{-1}. (2) Cross-exchange reactions with redox couples that are not able to form inner-sphere bridges (such as $Ru(NH_3)_6^{3+,2+}$) are slower and give average outer-sphere k_{11} values of 0.1 M^{-1} s^{-1} for several systems.[35] (3) In cases where a water molecule can act as a bridging ligand, the k_{11} values fall between these extremes.[19,20] The k_{11} values for Ni(III,II) complexes of tripeptideamides are as large as 1.2 (±0.2) $\times 10^5$ M^{-1} s^{-1}, whereas most tripeptides have k_{11} values of 1.3 (±0.1) $\times 10^4$ M^{-1} s^{-1}. These values are 10^5–10^6 times greater than those expected for outer-sphere electron transfer; therefore, an axial (z axis) water bridge between the Ni(III) and Ni(II) metal centers is proposed.[20] The water bridge assists the electron transfer from the d_{z^2} orbital of Ni(II) to the d_{z^2} orbital of Ni(III). The Aib_3 complex hinders this type of interaction but does not prevent some enhancement of the electron-transfer process.[20] Thus, the k_{11} value of 450 M^{-1} s^{-1} measured in this work is a factor of 30 smaller than that estimated for other tripeptides, but it is still 4.5×10^3 larger than the value calculated for outer-sphere processes.

Effect of Pyridine. Figure 3 gives the frozen aqueous solution EPR spectra of $Ni^{III}(H_{-2}Aib_3)$ obtained from solutions with and without pyridine present. Spectrum 3a is for $Ni^{III}(H_{-2}Aib_3)(H_2O)_2$, which was obtained from freezing a solution initially at pH 3.3 in the absence of pyridine. Spectrum 3b was obtained from freezing a solution initially at pH 6.5 with 0.05 M pyridine. The three-line splitting in $g_\parallel$ is typical for a complex with one ^{14}N nucleus along the z axis, and the spectrum corresponds to $Ni^{III}(H_{-2}Aib_3)(py)(H_2O)$. Spectrum 3c was obtained from freezing a solution initially at pH 6.5 with 1.25 M pyridine. The five-line (1:2:3:2:1) splitting in $g_\parallel$ corresponds to $Ni^{III}(H_{-2}Aib_3)(py)_2$ with two equivalent pyridines coordinated axially. Although the bis(pyridine) complex is observed in the frozen state, only the mono(pyridine) complex is found in aqueous solution.[36]

(30) Espenson, J. H. *Chemical Kinetics and Reaction Mechanisms*; McGraw-Hill: New York, 1981; pp 50–55.
(31) Caceci, M. S.; Catheris, W. P. *Byte* **1984**, *9*, 340–362.
(32) Yarboro, L. A.; Deming, S. N. *Anal. Chim. Acta* **1974**, *73*, 391–398.
(33) Bevington, P. R. *Data Reduction and Error Analysis for the Physical Sciences*; McGraw-Hill: New York, 1969; pp 66–118.
(34) Dennis, C. R.; Nemeth, M. T.; Kumar, K.; Margerum, D. W. To be submitted for publication.
(35) Kumar, K.; Margerum, D. W. To be submitted for publication.
(36) Murray, C. K.; Margerum, D. W. *Inorg. Chem.* **1982**, *21*, 3501–3506.

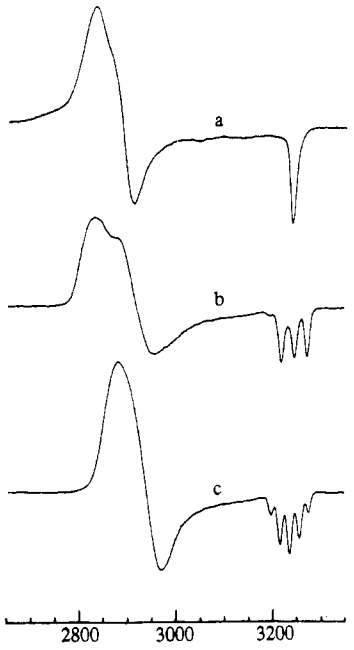

Figure 3. Frozen aqueous solution EPR spectra of Ni(III) complexes (2.98×10^{-4} M) at −150 °C, 9.08 GHz: (a) $Ni^{III}(H_{-2}Aib_3)(H_2O)_2$, pH 3.32; (b) $Ni^{III}(H_{-2}Aib_3)$ in the presence of 0.05 M $[py]_T$ at pH 6.50; (c) $Ni^{III}(H_{-2}Aib_3)$ in the presence of 1.25 M $[py]_T$ at pH 6.50.

Table III. Electron-Transfer Reactions of $Ni^{III,II}(H_{-2}Aib_3)^{0,-}$ in the Presence of Pyridine[a]

10^3C_A, M	10^3C_X, M	$[py]_T$, M	$k_{11(obsd)}$,[b] M^{-1} s^{-1}
0.376	1.35	0.150	160 ± 20
0.382	1.35	0.250	134 ± 5
0.384	1.35	0.333	129 ± 9
0.384	1.35	0.500	118 ± 6

[a] 23 ± 1 °C, μ = 0.1, magnetic field at 3045 G, pH ≃6.50. (The pK_a of pyridine is 5.24 at ± = 0.1: Smith, R. M.; Martell, A. E. *Critical Stability Constants*; Plenum Press: New York, 1975; Vol. 2, pp 165–166.) [b] Uncertainties are one standard deviation.

The axial waters in $Ni^{III}(H_{-2}Aib_3)(H_2O)_2$ are labile, and the freezing process greatly shifts the equilibrium to favor the coordination of ligands in solution. This is true for NH_3, imidazole, and chloride ion, as well as for pyridine. Electrochemical methods were used to measure an equilibrium constant of 40 ± 2 M^{-1} for K_1 in eq 7, and no evidence was found for a bis complex at room temperature.[36]

$$Ni^{III}(H_{-2}Aib_3)(H_2O)_2 + py \overset{K_1}{\rightleftharpoons} Ni^{III}(H_{-2}Aib_3)(py)(H_2O) \quad (7)$$

The rate of electron transfer between Ni(III) and Ni(II) decreases when pyridine is present in the solution. The ^{61}Ni effect on the EPR signal is used to monitor the reaction at 3045 G and gives the results in Table III. The $k_{11(obsd)}$ values decrease by a factor of 4 as the pyridine concentration increases (Figure 4) but level off as the free pyridine concentration approaches 0.5 M. The initial decrease can be attributed to the formation of the mono(pyridine) complex (eq 7), which is less favorable for electron transfer because the square-planar $Ni^{II}(H_{-2}Aib_3)^-$ complex shows no evidence of a pyridine adduct. The limiting rate constant at high pyridine concentration necessitates another electron-transfer path (k_{22}) by the pyridine complex (eq 8). This equation is an

$$^{61}Ni^{III}(H_{-2}Aib_3)(py)(H_2O) + Ni^{II}(H_{-2}Aib_3)^- \overset{k_{22}}{\rightleftharpoons} {}^{61}Ni^{II}(H_{-2}Aib_3)^- + Ni^{III}(H_{-2}Aib_3)(py)(H_2O) \quad (8)$$

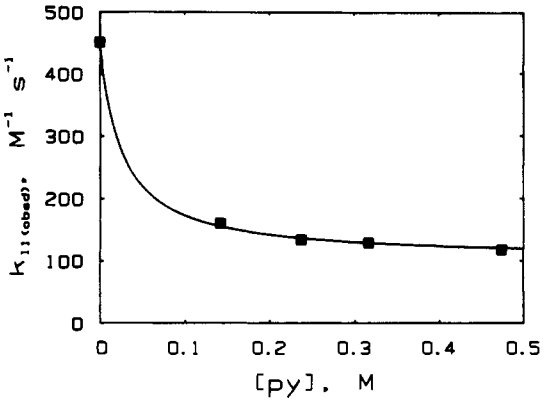

Figure 4. Dependence of $k_{11(obsd)}$ on pyridine concentration for $Ni^{III,II}(H_{-2}Aib_3)^{0,-}$. The solid line is calculated from eq 10 and data in Tables II and III.

abbreviated expression of a more complex process, where pyridine molecules are rapidly lost from the initial $^{61}Ni(II)$ species formed after electron transfer and pyridine rapidly adds to the Ni(III) species formed after electron transfer. The resulting exchange rate of the reaction is given by eq 9, where $[^{61}Ni^{III}]_T = [^{61}Ni^{III}(H_{-2}Aib_3)(H_2O)_2] + [^{61}Ni^{III}(H_{-2}Aib_3)(py)(H_2O)]$ and $k_{11(obsd)}$ fits eq 10. Figure 4 shows the fit of eq 10 for k_{11} = 450

$$R_{ex} = k_{11(obsd)}[^{61}Ni^{III}]_T[Ni^{II}(H_{-2}Aib_3)^-] \quad (9)$$

$$k_{11(obsd)} = \frac{k_{11} + k_{22}K_1[py]}{1 + K_1[py]} \quad (10)$$

M^{-1} s^{-1}, K_1 = 40 M^{-1}, and k_{22} = 103 ± 8 M^{-1} s^{-1}. Thus, the electron transfer takes place by parallel paths (eq 1 and 8), and the observed exchange rate constant is a combination of these two paths. High pyridine concentration forces the exchange process to proceed by eq 8. The axially coordinated pyridine blocks one water-bridging pathway but still permits a Ni(III)–H_2O–Ni(II) bridge from the opposite side of the complex. Even with a coordinated pyridine, the exchange rate constant is much larger than the values observed for an outer-sphere electron transfer.[35]

Conclusions

A new EPR method for the direct determination of electron-transfer rate constants of Ni(III,II) complexes has been developed. The limitations of the EPR/stopped-flow mixing system and the EPR signal-to-noise ratio impose a half-life requirement of greater than 4×10^{-2} s. Self-exchange rate constants as large as 10^4 M^{-1} s^{-1} can be measured by this technique. Any Ni(III,II) couple could be studied provided the EPR line widths of the $^{61}Ni(III)$ complex and the Ni(III) complex are different. It may be possible to extend the technique to other metal ion complexes such as iron, ruthenium, and chromium. One of the oxidation states of the metal must give an aqueous EPR spectrum, and an isotope must be available that has a different nuclear spin. Enriched ^{57}Fe (2.1% natural abundance, $I = {}^1/_2$) might be used with ^{56}Fe (91.8%, I = 0) and ^{54}Fe (5.8%, I = 0). Enriched ^{99}Ru (12.7%, $I = {}^5/_2$) or ^{101}Ru (17.1%, $I = {}^5/_2$) might be used because the other stable isotopes have no nuclear spin. Enriched ^{53}Cr (9.5%, $I = {}^3/_2$) might be used because the other stable Cr isotopes have no nuclear spin. All of these metal ions have oxidation states that generate EPR spectra, although some are easier to observe than others.

Acknowledgment. This work was supported by National Science Foundation Grants CHE-8319935 and CHE-8720318 and by Public Health Service Grant GM-12152 from the National Institute of General Medical Sciences.